

# Crystal Structures of the Multispecific 17 $\beta$ -Hydroxysteroid Dehydrogenase Type 5: Critical Androgen Regulation in Human Peripheral Tissues

WEI QIU, MING ZHOU, FERNAND LABRIE, AND SHENG-XIANG LIN

*Oncology and Molecular Endocrinology Research Center, Centre Hospitalier de l'Université Laval Medical Center (CHUL) and Laval University, Quebec, Canada G1V 4G2*

Human type 5 17 $\beta$ -hydroxysteroid dehydrogenase (17 $\beta$ -HSD5;AKR1C3) plays a major role in the metabolism of androgens in peripheral tissues. In prostate basal cells, this enzyme is involved in the transformation of dehydroepiandrosterone into dihydrotestosterone, the most potent androgen. It is thus a potential target for prostate cancer therapy because it is understood that the testosterone formation by this enzyme is an important factor, particularly in patients who have undergone surgical or medical castration. Here we report the first structure of a human type 5 17 $\beta$ -HSD in two ternary complexes, in which we found that the androstenedione molecule has a different binding position from that of testosterone. The two testoster-

one-binding orientations in the substrate-binding site demonstrate the structural basis of the alternative binding and multispecificity of the enzyme. Phe306 and Trp227 are the key residues involved in ligand recognition as well as product release. A safety belt in the cofactor-binding site enhances nicotinamide adenine dinucleotide phosphate binding and accounts for its high affinity as demonstrated by kinetic studies. These structures have provided a dynamic view of the enzyme reaction converting androstenedione to testosterone as well as valuable information for the development of potent enzyme inhibitors. (*Molecular Endocrinology* 18: 1798–1807, 2004)

HUMAN 17 $\beta$ -HYDROXYSTEROID dehydrogenase (17 $\beta$ -HSD) interconvert 17-ketosteroids and 17-hydroxysteroids using nicotinamide adenine dinucleotide phosphate (NADP) as a cofactor *in vitro*. They are responsible for the last step in the synthesis and the first step in the inactivation of all sex steroid hormones. Because the intracellular hormones play essential roles in many biological activities throughout human life, it is of major importance to study the detailed structure-function relationship of enzymes in this family. To date, 12 types of 17 $\beta$ -HSDs have been cloned and identified from different sources and species (1–15). The members of this family share a low sequence identity of around 17% (16) and each of them plays a specific role in the biosynthesis or inactivation of different steroid hormones in a tissue-specific manner. Among these enzymes, only one three-dimensional structure, that of the estrogenic human type 1 17 $\beta$ -HSD has been reported (17–19), and a potent inhibitor with nanomolar level affinity has been designed based on the structural information (20).

Abbreviations: DHEA, dehydroepiandrosterone; DHT, 5 $\alpha$ -dihydrotestosterone; 3 $\beta$ -HSD1, 3 $\beta$ -hydroxysteroid dehydrogenase; 17 $\beta$ -HSD, 17 $\beta$ -hydroxysteroid dehydrogenase; NADP, nicotinamide adenine dinucleotide phosphate; PDB, protein data bank; T-A, first testosterone; T-B, second testosterone.

***Molecular Endocrinology* is published monthly by The Endocrine Society (<http://www.endo-society.org>), the foremost professional society serving the endocrine community.**

In males, testosterone is normally produced by Leydig cells of the testes and secreted into the plasma. Testosterone is also carried to Sertoli cells of the testes, where it is converted into 5 $\alpha$ -dihydrotestosterone (DHT). Both testosterone and DHT are transported in the plasma and delivered to target tissues. DHT is the most potent androgen and is the key factor in many male hormone-related diseases, such as prostate cancer (21). Testosterone can also be converted to DHT in a number of peripheral target tissues. A crucial observation from prostate cancer studies was that, about 50% of DHT remained in the prostate of patients whose testicles had been surgically removed or were functionally blocked from secreting testosterone (22). This observation showed that the remaining DHT in the prostate after castration is synthesized from sources other than testosterone of testicular origin. To block testicular and adrenal sources of androgens, combination therapy using a LH-releasing hormone agonist and a pure antiandrogen was developed and has been widely used in advanced prostate cancer patients. This led to the first demonstration of life prolongation in prostate cancer patients (23, 24) and the proposal of the mechanism of intracrine sex hormone synthesis in peripheral tissues (25–28).

It is now well established that the prostatic tissue efficiently transforms the inactive steroid precursor dehydroepiandrosterone (DHEA) into the active androgen DHT. Further research using *in situ* hybridization and immunocytochemistry indicated that the DHT remaining in the prostate after castration can be synthe-

sized locally from DHEA by the concerted action of three enzymes, namely, type 1 3 $\beta$ -hydroxysteroid dehydrogenase (3 $\beta$ -HSD1), 17 $\beta$ -HSD5, and type 2 5 $\alpha$ -reductase (29). As shown in Fig. 1A,  $\Delta$ 4-androstene-3,17-dione (4-dione) is synthesized from DHEA by 3 $\beta$ -HSD1 in the basal cells; 17 $\beta$ -HSD5 then carries out the local conversion of 4-dione into testosterone; and finally, DHT is synthesized from testosterone by type 2 5 $\alpha$ -reductase in either the basal cells or the luminal cells of the prostate. DHT then binds to androgen receptors in the nuclei of luminal cells where prostate cancer originates. The major role of 17 $\beta$ -HSD5 in testosterone biosynthesis has also been demonstrated in the human ovary (30), abdominal visceral adipose tissue (31), and skin (32). The strategy of inhibitor design for this enzyme has also been studied (33). The blockage of 17 $\beta$ -HSD5 activity can interrupt this androgen formation chain and thereby substantially eliminate the intracrine synthesis of androgens in human peripheral tissues (29). The inhibitors may thus contribute to the treatment of prostate cancer or benign prostate hyperplasia, frequently found in aged men.

*In vitro*, homogeneous recombinant 17 $\beta$ -HSD5 expressed in *Escherichia coli* functions as a 3-keto, 17-keto, and 20-ketosteroid reductase and as a 3 $\alpha$ -, 17 $\beta$ -, and 20 $\alpha$ -hydroxysteroid oxidase. All the available results in the literature demonstrate the characteristic multispecificity of the enzyme. From kinetic studies *in vitro*, Penning *et al.* (34) reported that this enzyme prefers androgen inactivation as a reductase. In the same study, they also pointed out that the ability of the enzyme to make testosterone may be more

important in individuals who have undergone castration for the treatment of prostate cancer, which is in agreement with the report of El-Alfy *et al.* (29). Under such circumstances where testicular sources of androgens are absent, the physiological role of this enzyme in prostatic tissues favors the androgen biosynthesis pathway as shown in Fig. 1A.

The multispecificity of 17 $\beta$ -HSD5 raises questions concerning how the enzyme can selectively recognize different substrates and whether these substrates bind to the same site. The answers to these questions have awaited the determination of the first 3D-structure of 17 $\beta$ -HSD5, which will provide a better understanding of the substrate recognition and multispecificity of this important enzyme.

## RESULTS AND DISCUSSION

### Overall Structure

The structure of 17 $\beta$ -HSD5 was determined in two ternary complexes: 17 $\beta$ -HSD5/4-dione/NADP (P6<sub>3</sub> space group, 1 monomer/asymmetric unit, 42% solvent content) and 17 $\beta$ -HSD5/testosterone/NADP (P2<sub>1</sub> space group, 1 monomer/asymmetric unit, 45% solvent content). The overall structure is similar to the other structures in the aldo-keto reductase family (35). The 17 $\beta$ -HSD5 structure has an eight-stranded  $\alpha/\beta$  barrel in its center, a typical folding motif in a large family of enzymes, with each inner  $\beta$ -strand connected to an outer  $\alpha$ -helix. In addition, two  $\beta$ -strands

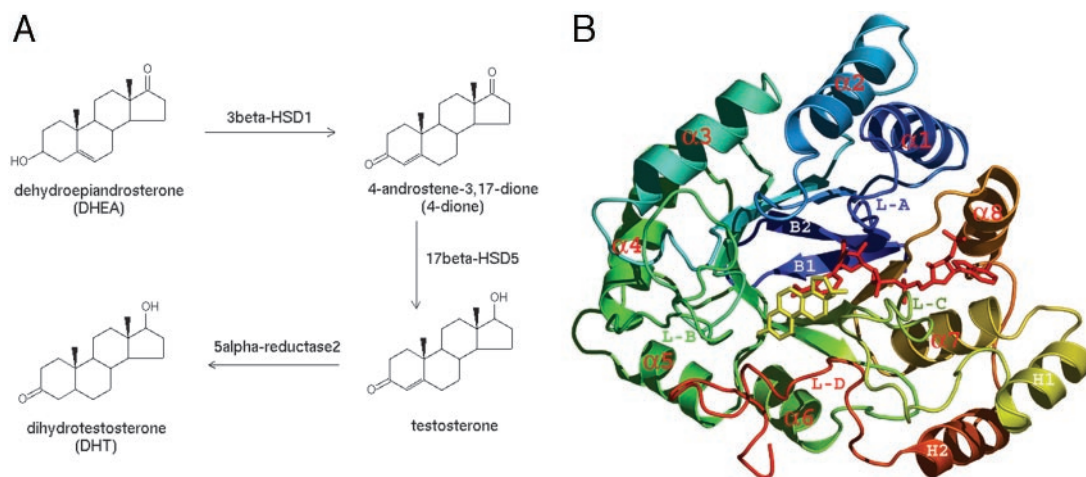


**Fig. 1.** The Role of 17 $\beta$ -HSD5 in the Androgen Formation and its Overall Structure

A, Schematic representation of DHT local formation in the peripheral tissues. 17 $\beta$ -HSD5 is involved in the conversion from 4-dione to testosterone: 1) 4-dione is synthesized from DHEA by 3 $\beta$ -HSD1 in the basal cells; 2) 17 $\beta$ -HSD5 then carries out the local conversion of 4-dione into testosterone; 3) DHT is synthesized from testosterone by type 2 5 $\alpha$ -reductase in either the basal cells or the luminal cells of the prostate. B, The cartoon representation of 17 $\beta$ -HSD5/testosterone/NADP structure. The testosterone molecule is displayed in *yellow stick* and NADP molecule in *red stick*. Two  $\beta$ -strands (B1 and B2, colored in *deep blue*) form a  $\beta$ -hairpin turn at the N terminus of the  $\beta$ -barrel; Two additional  $\alpha$ -helix (H1 and H2) are colored in *yellow* and *brown*. Four large loops, namely loop-A (L-A, *blue*), loop-B (L-B, *green*), loop-C (L-C, *light green*), and loop-D (L-D, *red*), form the substrate and cofactor-binding sites at the C-terminal end of the  $\alpha/\beta$  barrel. All figures are generated with program PyMOL (DeLano, W. L., 2002; <http://www.pymol.org>).

(B1 and B2) form a  $\beta$ -hairpin turn preceding  $\beta$ 1 of the barrel, blocking the N terminus of the  $\beta$ -barrel; one  $\alpha$ -helix (H1) interrupts between  $\alpha$ 7 and  $\beta$ 8 and another one (H2) follows  $\alpha$ 8 at the C terminus. Four large loops, namely loop-A (residue 24–33), loop-B (residue 117–143), loop-C (residue 217–238), and loop-D (residue 301–323), help to form the substrate and cofactor-binding site at the C-terminal end of the  $\alpha/\beta$  barrel (Fig. 1B). In addition, the refined models from the two ternary complexes have a root mean squared deviation of 0.61 Å for 311 C $\alpha$  atoms from the enzyme protein and a maximum deviation of 3.1 Å at C $\alpha$  of Gly315. The differences between the two forms are mainly associated with those residues located in the above-mentioned four loops and some residues at the N-terminal. The cofactors in the two structures are located in the same position with identical conformations. However, the substrates adopt two significantly different conformations as shown in Fig. 2.

#### Different Binding Modes for Testosterone and 4-Dione

17 $\beta$ -HSD5 has a very hydrophobic substrate-binding pocket. The nicotinamide ring of NADP and 17 residues, most of which are aromatic residues (Tyr24, Leu54, Tyr55, Trp86, His117, Ser118, Pro119, Met120, Ser129, Asn167, Phe306, Ser308, Ser310, Phe311, Tyr317, Pro318, and Tyr319), form an elliptical cavity at the C-terminal end of the barrel. Many of these aromatic residues have their side chains oriented toward the binding pocket. As shown in Fig. 2, the substrate and cofactor-binding sites of 17 $\beta$ -HSD5 are located deep inside the enzyme. In the 17 $\beta$ -HSD5/4-dione/NADP structure (Fig. 2A), the substrate-binding site is compact and narrow. The entry for substrate-binding is relatively small and has a scalene triangular form. The volume of this cavity is about 450 Å<sup>3</sup>. In the 17 $\beta$ -HSD5/testosterone/NADP structure (Fig. 2B), the substrate-binding pocket is open to the surface with the substrate (testosterone) lying toward the cofactor-binding site. The volume of the cavity for testosterone binding is much bigger than that for 4-dione (~790 Å<sup>3</sup>). The hydrophobicity and flexibility of this pocket are designed for the binding of different steroids. The substrate binding pocket we observed in 17 $\beta$ -HSD5 is much closer to the protein surface and less compact than that for estrogen in type 1 17 $\beta$ -HSD [protein data bank (PDB) code: 1IOL]. Similar comparison is found between 17 $\beta$ -HSD5 and androgen receptor (PDB code: 1E3G), the latter has a narrow ligand binding pocket deeply engulfed in the enzyme protein.

In the 4-dione complex, a close look at the substrate binding site reveals that the substrate is oriented with the 17-keto position toward the center of the enzyme. The steroid plane is almost perpendicular to the plane of the nicotinamide ring of NADP with its  $\beta$ -face toward the cofactor. On the other side, the  $\alpha$ -face of the steroid plane leans nicely on a flat surface in the bind-

ing site, with the side chain of Phe311 stacking against it. The 4-dione molecule binds deeply in the interior of the barrel with the whole D-ring on the A-face of the nicotinamide ring. The distance between the 17-keto group of 4-dione and the C4 of the nicotinamide ring of NADP is 7.2 Å. This indicates that the 4-dione position obtained from the crystal structure is not in the catalytic position.

In the 17 $\beta$ -HSD5/testosterone/NADP complex, two testosterone molecules could be identified at the same binding site with different orientations (Fig. 3). The density of the  $\sigma$ -A weighted 2Fo-Fc map in the substrate-binding site is a composite of two testosterone molecules oppositely oriented with occupancy of the first testosterone (T-A) of 65% and the second (T-B) of 35%. This result was double-checked by the omit map in which both ligand molecules and the amino acids within a 5-Å distance were omitted. Under experimental conditions, it turns out to be more stable for testosterone to bind to the enzyme in a reversed binding mode, with O3 close to the catalytic site, as shown by the principle testosterone orientation (T-A) in Fig. 3A. In this case, with a 3-keto group that orients toward the cofactor, testosterone is supposed to mimic the substrate of 3 $\alpha$ -HSD. The two testosterone-binding orientations in the substrate-binding site demonstrate the structural basis of the alternative binding and multispecificity of the enzyme.

Due to the pseudo self-symmetry property in the steroid core, one can rotate the steroid plane about 180° around an axis near C9 of the steroid core and superimpose the A-ring to the D-ring and the B-ring to the C-ring (36) (Fig. 3B). In the substrate-binding site, a large portion of the electron densities can be shared by two testosterone molecules. O17 of T-A and O3 of T-B are almost superimposed, oriented toward the surface of the protein. Each of the two oxygen atoms forms two hydrogen bonds with two water molecules. The major deviations in the superimposed ligands are located in the O3 of T-A and O17 of T-B, as shown in Fig. 3B. Both oxygen atoms have a good electron density and each forms a strong hydrogen bond with O $\gamma$  of Ser118, O17 of T-B also forms a water-mediated hydrogen bond. These hydrogen bonds are believed to stabilize the conformation of testosterone in the crystal structure. In addition to these hydrogen-bonding interactions, testosterone has also strong hydrophobic interactions with the substrate-binding pocket. The conformations of all those amino acids that form the binding pocket remain the same for the two alternative binding modes.

As illustrated in Fig. 2C, in the complex of 17 $\beta$ -HSD5/testosterone/NADP, the steroid plane of T-A moves to its  $\beta$ -face, which is closer to the NADP-binding site, and forms an angle of about 35° with the steroid plane of 4-dione in the 17 $\beta$ -HSD5/4-dione/NADP complex. The conformations of the side chains of Phe306 and Trp227 in the two crystal forms are dramatically different. Instead of being located on the  $\beta$ -face of 4-dione, the side chains of Phe306 and

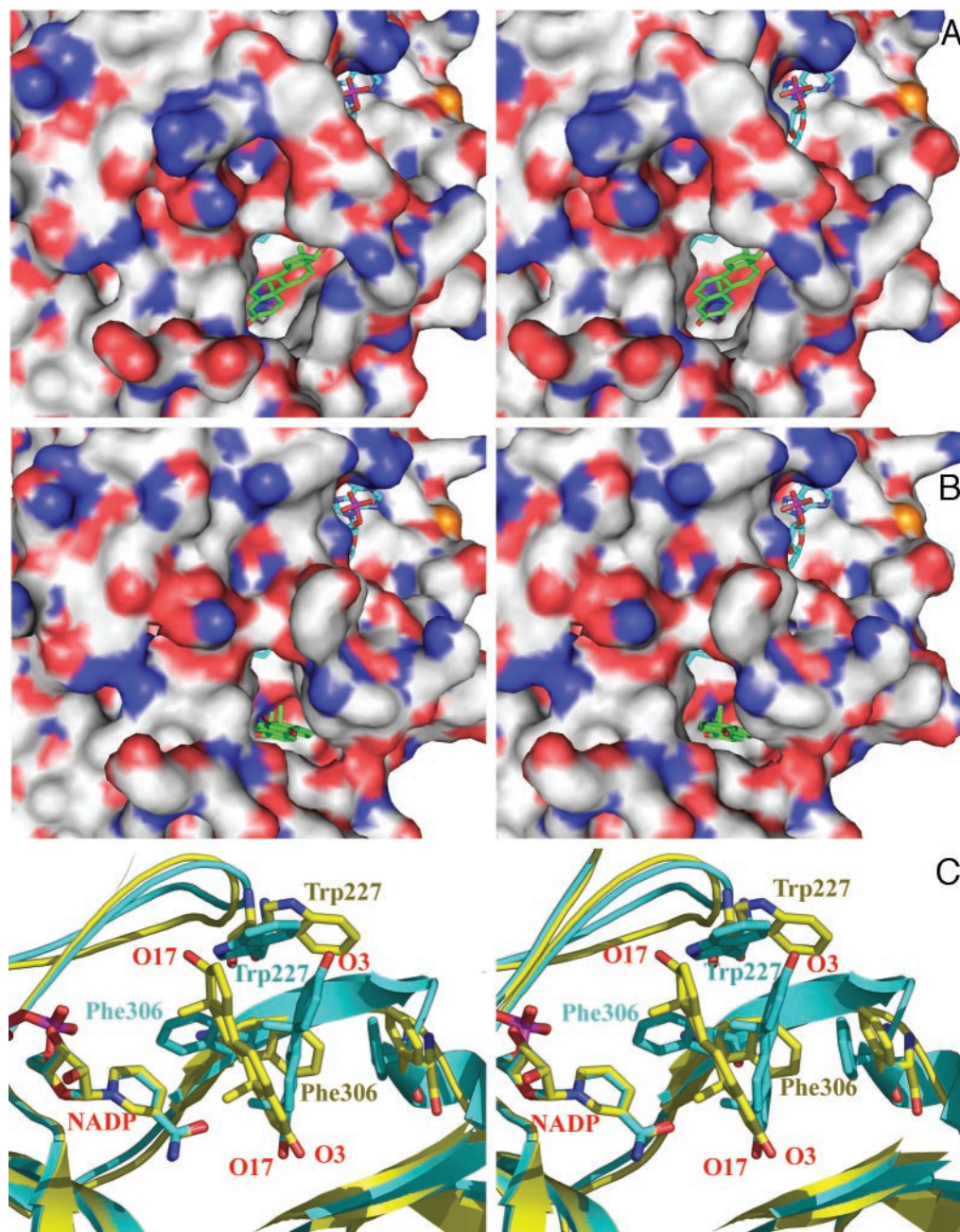


**Fig. 2.** Testosterone and 4-Dione Have Different Docking Positions at the 17 $\beta$ -HSD5 Substrate-Binding Site

A, The stereo view of the molecular surface at the substrate and cofactor binding site of 17 $\beta$ -HSD5/4-dione/NADP complex: 4-dione molecule is presented in *green sticks* and NADP in *cyan sticks*. The substrate-binding site is compact and narrow. The entry for substrate-binding is relatively small and has a *scalene triangular shape*. B, The stereo view of the molecular surface at the substrate and cofactor binding site of 17 $\beta$ -HSD5/testosterone/NADP complex: testosterone molecule is presented in *green sticks* and NADP in *cyan sticks*. Testosterone molecule is lying toward the cofactor-binding site. C, Superimposition of two ternary complexes structures at their substrate-binding sites. Arg226, Trp227 and Phe306 are located on the  $\alpha$ -face of testosterone and on the  $\beta$ -face of 4-dione (*yellow*, 17 $\beta$ -HSD5/testosterone/NADP; *cyan*, 17 $\beta$ -HSD5/4-dione/NADP). Note: to simplify the illustration, only one testosterone (T-A) from the 17 $\beta$ -HSD5/testosterone/NADP structure is shown in this figure as well as in Fig. 3A.

Trp227 are now located on the  $\alpha$ -face of the steroid core of testosterone, which forces the steroid to lie toward the cofactor binding site. In the 17 $\beta$ -HSD5/testosterone/NADP complex, the O17 of T-A and the O3 of T-B were found to be located in the region where

several hydrophilic amino acids (Ser221, Glu222, and Asp224) are grouped. At the other end of the steroid, O3 of T-A and O17 of T-B are close to the base of the substrate-binding pocket, and both form a strong hydrogen bond with O $\gamma$  of Ser118. In the 17 $\beta$ -HSD5/

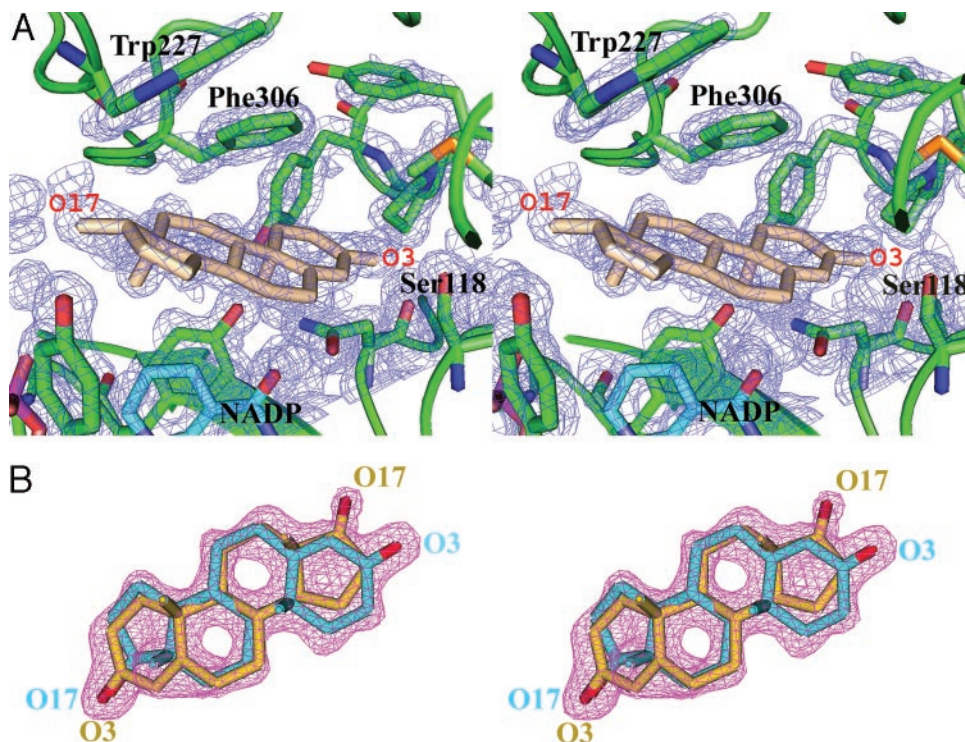


**Fig. 3.** The Two Testosterone-Binding Orientations in the Substrate-Binding Site Demonstrate the Structural Basis of the Alternative Binding and Multispecificity of the Enzyme

A, The stereo view of the substrate-binding site of 17 $\beta$ -HSD5/testosterone/NADP complex. Residue Trp227 and Phe306 are located on the  $\alpha$ -face of the steroid core of T-A, which forces the steroid to lie toward the cofactor binding site. O3 of T-A forms a strong hydrogen bond with O $\gamma$  of Ser118. The density is the  $\sigma$ -A weighted 2Fo-Fc map contoured at 1.0 $\sigma$ . B, The composite electron density for two testosterone molecules oriented oppositely in the substrate-binding site (T-A in cyan stick and T-B is brown stick). The density is the  $\sigma$ -A weighted 2Fo-Fc map contoured at 0.9 $\sigma$ .

testosterone/NADP complex, we also found that the N $\eta$ 2 of Arg226 forms a strong hydrogen bond (2.7 Å) with the O of Ala70 from a symmetrically related molecule, whereas in the 17 $\beta$ -HSD5/4-dione/NADP complex, Arg226 forms two salt bridges with Asp224 (3.1 Å) and Glu28 (2.8 Å) in the same molecule.

### Substrate Recognition

With the pseudo self-symmetry property of steroids (36), one can expect that 4-dione can enter into its binding with either the 17- or 3-positions toward the catalytic position. In the 17 $\beta$ -HSD5/4-dione/NADP structure we observed that due to steric hindrance 4-dione can only enter the binding site with the 17-keto position toward the catalytic position. The key amino acids, Phe306 and Trp227 play an important role in substrate recognition as demonstrated by this complex structure. As illustrated by Fig. 2A, the entrance to the substrate-binding site has a scalene triangular form that adapts to the shape of the C19-steroid. The side chains of Phe306 and Trp227 swing toward the wall of the substrate-binding site, which allows easy access of the substrate to the area with its O17 close to the nicotinamide ring of NADP, where the reaction occurs. The distances between C18 of 4-di-

one and the benzene ring of Phe306, C19 of 4-dione and the benzene ring of Phe306, C19 of 4-dione and Trp227 are all around 4–5 Å. If the substrate had entered the binding site with 3-keto pointing toward the enzyme, we would expect to encounter steric hindrance between C18 and C19 of the substrate and the side chains of Phe306 and Trp227. In the model with a reversed 4-dione, C18 would be 3.2 Å from the side chain of Phe306 and C19 would be 3.7 Å from the side chain of Trp227. This means that in the case of the reversed 4-dione binding mode, the side chains of Phe306 and Trp227 need to shift further toward the wall of the substrate-binding site to lead the 3-keto of 4-dione to the catalytic region. In fact, it was shown in our kinetic studies that testosterone is the only product formed when initial velocities were measured with 4-dione as the substrate, thereby demonstrating that 4-dione can access the binding site correctly to be catalyzed.

### NADP-Binding Site

In both ternary complex structures, the NADP molecule was well defined at approximately the same binding position with an unusual extended conformation across the ( $\alpha/\beta$ )<sub>3</sub> barrel. The nicotinamide ring of

NADP is located at the bottom of the active site, which makes the hydrogen of C4N accessible from the substrate. A strong network of hydrogen bonds and charged-coupling interactions were found between NADP and residues Tyr24, Asp50, Ser166, Asn167, Gln190, Ser217, Ser221, Lys270, Ser271, Arg276, Gln279, and Asn280 of the enzyme. Interestingly, a safety belt was found at the NADP-binding site. Residue Glu222 from the flexible loop-C bends over the pyrophosphate of NADP and forms two salt links with N $\zeta$  of Lys270 from  $\beta$ -strand 266–271 (3.1 Å) and the carboxylic oxygen of Tyr24 from  $\beta$ -strand 19–24 (2.9 Å) (Fig. 4). This safety belt seems to shift the loop-C much closer to the cofactor, significantly enhancing the cofactor affinity. This is strongly supported by the steady-state kinetic assay, which has shown a  $K_m$  of 7.1 nM for NADP in the oxidation reaction.

The safety belt is absent in structures of rat 3 $\alpha$ -HSD (38), human 3 $\alpha$ -HSD3 (39), and human 20 $\alpha$ -HSD (40). Comparing the amino acid sequences surrounding the cofactor-binding site in the rat 3 $\alpha$ -HSD, human 3 $\alpha$ -HSD3, human 20 $\alpha$ -HSD, and human 17 $\beta$ -HSD5 enzymes, we find that the key substitution for the cofactor-binding site among these structures is at position 222. In the rat 3 $\alpha$ -HSD enzyme, the side chain of Ser222 is too short to form a hydrogen bond with Arg270 or Tyr24. Similarly, His 222 in human 3 $\alpha$ -HSD3 and 20 $\alpha$ -HSD is also unable to form a bond with Lys270 because the nitrogen atoms in the side chains of His222 and Lys270 are hydrogen bond donors but not acceptors. As a result, the side chain of His222 is shifted toward the substrate-binding pocket thus affecting substrate binding.

#### A Dynamic Model for the Enzyme Reaction

From the above described crystal structures of 17 $\beta$ -HSD5 in the two complexes, we propose a model that

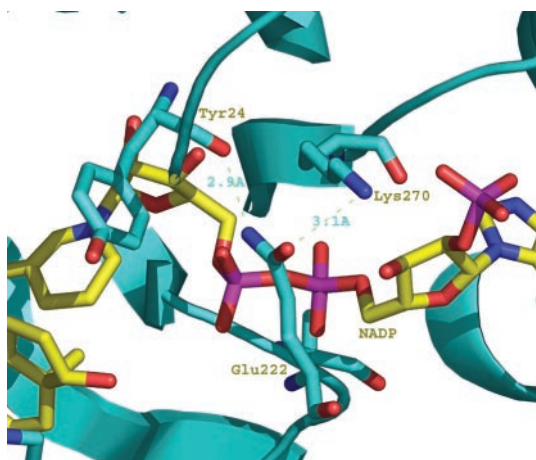


**Fig. 4.** Safety Belt in NADP-Binding Site

Residue Glu222 from the flexible loop-C bends over the pyrophosphate of NADP and forms two salt links with N $\zeta$  of Lys270 from  $\beta$ -strand 266–271 (3.1 Å) and the carboxylic oxygen of Tyr24 from  $\beta$ -strand 19–24 (2.9 Å).

may interpret the conversion of 4-dione into testosterone by 17 $\beta$ -HSD5. First, from the crystal structures, we found two tunnels that were well designed for substrate entry (4-dione in 17 $\beta$ -HSD5/4-dione/NADP complex) and product release (testosterone in 17 $\beta$ -HSD5/testosterone/NADP). The entrance tunnel is formed by loop-B, loop-C, and loop-D. This is the most accessible area from the surface to the substrate-binding site, as shown in Fig. 1B and 2A. The releasing tunnel is located between loop-A and loop-C, at the bottom where the NADP cofactor lies, as shown in Figs. 1B and 2B.

Recognized by Phe306 and Trp227, 4-dione can enter the substrate-binding site through the entrance tunnel with the 17-keto position toward the center of the enzyme. Under normal catalytic conditions, the conversion of 4-dione to testosterone occurs at the catalytic site near the nicotinamide ring of NADPH. The reaction induces conformational changes in both the nicotinamide ring of NADPH and the D-ring of the steroid and these conformation changes force the steroid to move away from the catalytic site. The product of this reaction, testosterone, has then to reposition itself in the substrate-binding site after reaction. The new position of testosterone can be demonstrated in the 17 $\beta$ -HSD5/testosterone/NADP complex structure. The 17-hydroxy group of the steroid forms a hydrogen bond with O $\gamma$  of Ser118, immobilizing the position at the D-ring end and allowing movement only at the end of the A-ring. As shown in Fig. 2C, the steroid plane of testosterone rotates toward its  $\beta$ -face for about 35° from the original substrate-binding position. In this structure, the O3-keto of T-B is also stabilized by two solvent-induced hydrogen bonds. At the same time, the side chains of Trp227 and Phe306 are forced to swing to the  $\alpha$ -face of testosterone to accommodate the repositioning of the steroid. Loop-C also moves closer to the substrate entrance tunnel than in the 17 $\beta$ -HSD5/4-dione/NADP structure. Most side chain conformations at this stage are believed to be close to those that we observed in the 17 $\beta$ -HSD5/testosterone/NADP structure.

The conformational changes of Trp227 and Phe306 can trigger the product release. As we mentioned before, Trp227 and Phe306 are the key amino acids for substrate recognition. The side chains of these two residues are located on the  $\alpha$ -face of testosterone after the reaction occurs (shown in the 17 $\beta$ -HSD5/testosterone/NADP structure). This is not their favorite conformation and they tend to turn toward the inside of the enzyme molecule. This movement can result in the breaking of the hydrogen bond formed between the 17-OH of testosterone and the O $\gamma$  of Ser118. These two residues further push testosterone toward its releasing tunnel. This tunnel consists of two flexible loops, loop-A and loop-C, which also form a short tunnel for the pyrophosphate bridge of the NADP. The release of testosterone could induce a series of conformational changes in loop-C that makes the breaking of the safety belt for NADP binding.

It has been reported that 17 $\beta$ -HSD5 functions as a dual pyridine nucleotide-specific reductase and catalyzes an ordered bi-bi mechanism, in which steroid substrate binds to the enzyme after the cofactor, whereas the steroid product releases from the enzyme before the cofactor (41). As shown in the rat liver 3 $\alpha$ -HSD apoenzyme structure (42) (PDB code: 1RAL) and with the NADP binary complex structure (43) (PDB code: 1LWI), the loop-C stays away from the center of the barrel, leaving the cofactor binding site open to the solvent surface. From our two ternary complexes, we suggest that the movement of this loop may permit the cofactor to enter and to be released from its binding site. When NADPH binds to the enzyme, it mediates a strong network of hydrogen bonds and charge-coupling interactions with some residues from the barrel and loop-C. These interactions turn the loop toward the center of the barrel. As a result, Glu222 from this loop forms the safety belt with the two residues, Lys270 and Tyr24, that are located in two  $\beta$ -strands from the core  $\alpha/\beta$  barrel motif. The safety belt further tightens the cofactor binding. The dissociation of NADP would require a conformational change that can be initiated by the release of the product as described above.

### Divergent Evolution

It has been pointed out that the  $\alpha/\beta$  barrel enzymes may have diverged from a common ancestor, based on structural and chemical evidence (35). Sequence comparison of the four HSD enzymes from the aldoketo reductase family shows that 17 $\beta$ -HSD5 shares 69.6%, 87.9%, and 87.8% sequence identities with rat 3 $\alpha$ -HSD, human 3 $\alpha$ -HSD3, and human 20 $\alpha$ -HSD, re-

spectively. Rat liver 3 $\alpha$ -HSD apoenzyme structure (42), its binary complex structure with NADP (43) and its ternary complex with testosterone and NADP (38) have been reported. Human type 3 $\alpha$ -HSD ternary structure with testosterone and NADP, and human 20 $\alpha$ -HSD ternary complex structure with 20 $\alpha$ -OH progesterone and NADP have also been solved (39, 40, 44). With the availability of all these structures, we can better compare the differences between the enzymes and look for their evolutionary relationship.

In the 17 $\beta$ -HSD5/testosterone/NADP complex structure, Ser118 plays an important role in substrate binding. The O $\gamma$  of Ser118 forms a strong hydrogen bond (2.6 Å) with the O3 of testosterone. This hydrogen bond allows testosterone to bind deeply at the base of the substrate-binding site. The corresponding residue to Ser118 in the other three enzymes is Phe118, a much bulkier amino acid than serine. In rat 3 $\alpha$ -HSD, human 3 $\alpha$ -HSD3, and human 20 $\alpha$ -HSD structures, Phe118 cannot form a hydrogen bond with the substrate, and it pushes testosterone much further toward the surface of the enzyme. The differences between the testosterone-binding positions in the human 17 $\beta$ -HSD5-testosterone-NADP complex and rat 3 $\alpha$ -HSD-testosterone-NADP complex are shown in Fig. 5.

The above comparison provides direct structural evidence to explain why only 17 $\beta$ -HSD5 has both significant 17-keto reductase and 17 $\beta$ -hydroxysteroid oxidase activities among the four enzymes previously mentioned, providing structural intracrine androgen formation evidence of a divergent evolution among this enzyme family. Although the establishment of the enzyme's major function requires a detailed study at the cellular level (41), these structures provide a strong

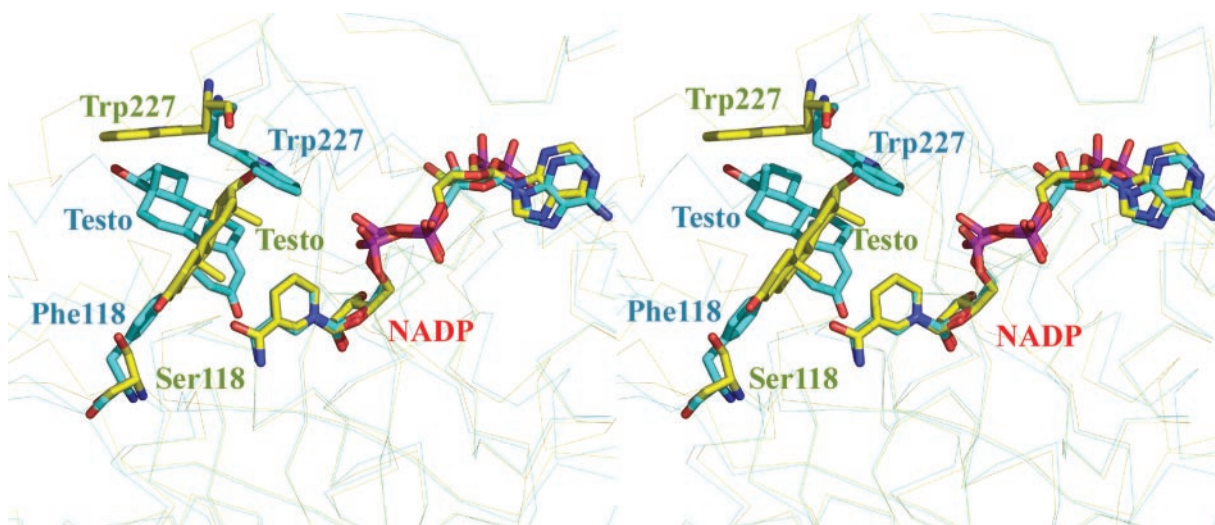


**Fig. 5.** Superimposition of Rat 3 $\alpha$ -HSD-Testosterone-NADP (Yellow) and Human 17 $\beta$ -HSD5-Testosterone-NADP (Cyan) Complexes

Ser118 of 17 $\beta$ -HSD5 allows testosterone to bind further into the base of the binding pocket by forming a strong hydrogen bond.

**Table 1.** Data Processing and Refinement Statistics of the 17 $\beta$ -HSD5/Testosterone/NADP and 17 $\beta$ -HSD5/4-Dione/NADP Complexes

Complex Form	17 $\beta$ -HSD5/Testosterone/NADP	17 $\beta$ -HSD5/4-Dione/NADP
Resolution range (Å)	30.0–1.32	30.0–2.0
Space group	P2 <sub>1</sub>	P6 <sub>3</sub>
Unit cell	a = 47.41; b = 77.16; c = 48.47 Å $\beta$ = 116.32°	a = 110.58; b = 110.58; c = 56.89 Å
R <sub>cryst</sub> /R <sub>free</sub> (%)	19.8/22.1	18.5/24.2
Number of atoms		
Protein (nonhydrogen)	2490	2529
Substrates	42	21
NADP	48	48
Cl <sup>-</sup>	2	N/A
Acetate	N/A	4
Water	345	275
RMS deviations		
Bonds (Å)	0.005	0.006
Angle (°)	1.25	1.24
Dihedrals angle (°)	22.04	21.80
Planarity (°)	0.88	0.82
Mean B factors (Å <sup>2</sup> )		
Protein main chain	16.2	17.8
Protein side chain	19.1	21.5
Substrates	22.8	36.0
NADP	12.6	14.3
Cl <sup>-</sup>	17.9	N/A
Acetate		30.5
Water	28.9	33.0

RMS, Root mean squared; N/A, not available; R<sub>cryst</sub>,  $\epsilon [Fo - Fc]/\epsilon Fo$ ; R<sub>free</sub>, calculated with 5% of data withheld from refinement.

basis for the study of the structure, function, and inhibition of this important enzyme.

## MATERIALS AND METHODS

### Purification and Crystallization

Human 17 $\beta$ -HSD5/GST was expressed in *E. coli*. The enzyme was purified using a GST column and a Blue Sepharose 6B column. Although the enzyme was reported to be highly labile (5), we were able to improve the recovery and specific activity of the enzyme using freeze-thaw disruption in the presence of 0.8%  $\beta$ -OG and the cofactor NADP. The purified protein was stable at 27 C for more than 1 wk. Before crystallization, the protein was concentrated to 20 mg/ml in its stock buffer. The vapor diffusion (hanging drop) method was used for enzyme crystallization. Two forms of crystals were obtained under the following crystallization conditions: 0.1 M Tris (pH 8.5), 0.2 M MgCl<sub>2</sub>, and 30% polyethylene glycol 3000, and 0.1 M sodium cacodylate (pH 6.5), 0.2 M magnesium acetate, and 20% polyethylene glycol 8000 in the reservoir solution (45). Although testosterone and NADP were present in both crystallization conditions, in the refined substrate-binding site we observed only 4-dione in the P6<sub>3</sub> form that was crystallized at pH 6.5, and testosterone in the P2<sub>1</sub> form that was obtained at pH 8.5.

### Evaluation of the Cofactor's Apparent Affinity

The apparent affinity of the cofactor was evaluated by the measurement of the cofactor K<sub>m</sub> of 17 $\beta$ -oxidation. The initial

reaction velocities were measured in the presence of a constant testosterone concentration (2  $\mu$ M) and NADP concentrations varying from 0.01–0.1  $\mu$ M at pH 7.5; the K<sub>m</sub> was then obtained from the Lineweaver-Burke reciprocal plot.

### Data Collection and Reduction

Two data sets were collected at 100K with monochromatic synchrotron radiation ( $\lambda$  = 0.95 Å) using a Quantum-4 CCD detector at the X-8 C beamline (Brookhaven National Laboratory, Upton, NY). Data were processed using the DENZO and SCALEPACK program (46). The processing statistics data are given in Table 1.

### Structure Solution and Refinement

Human 17 $\beta$ -HSD5 shares 69.9% sequence identity with rat 3 $\alpha$ -HSD, whose x-ray structure, in complex with testosterone and NADP, was solved to a resolution of 2.5 Å (38). The structure of 17 $\beta$ -HSD5 with a P6<sub>3</sub> space group was first solved using the rat 3 $\alpha$ -HSD structure as the search model (PDB code 1AFS). EPMR was used to carry out the molecular replacement (47). A correlation coefficient factor of 0.529 and an R-factor of 42.9% were obtained. The model for the P2<sub>1</sub> crystal was then obtained using the refined 17 $\beta$ -HSD5 model from the P6<sub>3</sub> structure as the search model. A correlation coefficient factor of 0.525 and an R-factor of 40.4% were obtained.

The models for 17 $\beta$ -HSD5 were auto rebuilt by one cycle of ARP-wARP (48) and subjected to multiple cycles of model rebuilding with program O (49) and refined with Refmac5 (50). The models for cofactors and substrates were carefully built into the densities based on the omit density map and  $\sigma$ -A weighted 2Fo-Fc map. The qualities of both structures were shown in Table 1.

An acetate molecule was also defined near the substrate and cofactor binding sites in the 17 $\beta$ -HSD5/4-dione/NADP



complex. Two chloride ions were defined near the substrate-binding site in the 17 $\beta$ -HSD5/testosterone/NADP complex. Water molecules were gradually added to the model by using the ARP-wARP program and then removed manually by the O program.

### Acknowledgments

The authors are thankful to Dr. V. Luu-The from CHUL research center for providing the *E. coli* cells overexpressing human 17 $\beta$ -HSD5. We appreciate the help from Dr. V. Nahoum and Dr. R. Shi from our laboratory for useful discussions.

Received January 26, 2004. Accepted April 7, 2004.

Address all correspondence and requests for reprints to: Sheng-Xiang Lin, Oncology and Molecular Endocrinology Laboratory, Laval University, 2705 Boulevard Laurier, Sainte-Foy, Quebec, Canada G1V 4G2. E-mail: sxlin@crchul.ulaval.ca.

We acknowledge the support from the Medical Research Council of Canada/Canadian Institutes of Health Research for 17 $\beta$ -HSD crystallography and the support of EndoRecherche in this project.

### REFERENCES

- Adamski J, Jakob FJ 2001 A guide to 17 $\beta$ -hydroxysteroid dehydrogenases. *Mol Cell Endocrinol* 171:1–4
- Brereton P, Suzuki T, Sasano H, Li K, Duarte C, Obeyesekere V, Haeseleer F, Palczewski K, Smith I, Komesaroff P, Krozowski Z 2001 Pan1b (17 $\beta$ -HSD11)-enzymatic activity and distribution in the lung. *Mol Cell Endocrinol* 22:111–117
- He XY, Merz G, Mehta P, Schulz H, Yang SY 1999 Human brain short chain L-3-hydroxyacyl coenzyme A dehydrogenase is a single-domain multifunctional enzyme. Characterization of a novel 17 $\beta$ -hydroxysteroid dehydrogenase. *J Biol Chem* 274:15014–15019
- Krazeisen A, Breitling R, Imai K, Fritz S, Moller G, Adamski J 1999 Determination of cDNA, gene structure and chromosomal localization of the novel human 17 $\beta$ -hydroxysteroid dehydrogenase type 7(1). *FEBS Lett* 29:373–379
- Dufort I, Rheault P, Huang X-F, Soucy P, Luu-The V 1999 Characteristics of a highly labile human type 5 17 $\beta$ -hydroxysteroid dehydrogenase. *Endocrinology* 140:1–7
- Su J, Lin M, Napoli JL 1999 Complementary deoxyribonucleic acid cloning and enzymatic characterization of a novel 17 $\beta$ /3 $\alpha$ -hydroxysteroid/retinoid short chain dehydrogenase/reductase. *Endocrinology* 140:5275–5284
- Fomitcheva J, Baker ME, Anderson E, Lee GY, Aziz N 1998 Characterization of Ke 6, a new 17 $\beta$ -hydroxysteroid dehydrogenase, and its expression in gonadal tissues. *J Biol Chem* 273:22664–22671
- Li KX, Smith RE, Krozowski ZS 1998 Cloning and expression of a novel tissue specific 17 $\beta$ -hydroxysteroid dehydrogenase. *Endocr Res* 24:663–667
- Nokelainen P, Peltoketo H, Vihko R, Vihko P 1998 Expression cloning of a novel estrogenic mouse 17 $\beta$ -hydroxysteroid dehydrogenase/17-ketosteroid reductase (m17HSD7), previously described as a prolactin receptor-associated protein (PRAP) in rat. *Mol Endocrinol* 12:1048–1059
- Biswas MG, Russel DW 1997 Expression cloning and characterization of oxidative 17 $\beta$ - and 3 $\alpha$ -hydroxysteroid dehydrogenases from rat and human prostate. *J Biol Chem* 272:15959–15966
- Khanna M, Qin KN, Wang RW, Cheng KC 1995 Substrate specificity, gene structure, and tissue-specific distribution of multiple human 3 $\alpha$ -hydroxysteroid dehydrogenases. *J Biol Chem* 270:20162–20168
- Geissler WM, Davis DL, Wu L, Bradshaw KD, Patel S, Mendonca BB, Elliston KO, Wilson JD, Russel DW, Andersson S 1994 Male pseudohermaphroditism caused by mutations of testicular 17 $\beta$ -hydroxysteroid dehydrogenase 3. *Nat Genet* 7:34–39
- Wu L, Einstein M, Geissler WM, Chan HK, Elliston KO, Andersson S 1993 Expression cloning and characterization of human 17 $\beta$ -hydroxysteroid dehydrogenase type 2, a microsomal enzyme possessing 20  $\alpha$ -hydroxysteroid dehydrogenase activity. *J Biol Chem* 268:12964–12969
- Luu-The V, Labrie C, Zhao H-F, Couet J, Lachance Y, Simard J, Leblanc G, Labrie F 1989 Characterization of cDNAs for human estradiol 17 $\beta$ -dehydrogenase and assignment of the gene to chromosome 17: evidence of two mRNA species with distinct 5'-termini in human placenta. *Mol Endocrinol* 3:1301–1309
- Peltoketo H 1988 Complete amino acid sequence of human placental 17 $\beta$ -hydroxysteroid dehydrogenase deduced from cDNA. *FEBS Lett* 239:73–77
- Peltoketo H, Luu-The V, Simard J, Adamski J 1999 17 $\beta$ -Hydroxysteroid dehydrogenase (HSD)/17-ketosteroid reductase (KSR) family; nomenclature and main characteristics of the 17HSD/KSR enzymes. *J Mol Endocrinol* 23:1–11
- Ghosh D, Pletnev VZ, Zhu D-W, Wawrzak Z, Duax W-L, Pangborn W, Labrie F, Lin S-X 1995 Structure of human 17 $\beta$ -hydroxysteroid dehydrogenase at 2.20 resolution. *Structure* 3:503–513
- Azzi A, Rehse PH, Zhu DW, Campbell RL, Labrie F, Lin S-X 1996 Crystal structure of human estrogenic 17 $\beta$ -hydroxysteroid dehydrogenase complexed with 17 $\beta$ -estradiol. *Nat Struct Biol* 3:665–668
- Breton R, Housset D, Mazza C, Fontecilla-Camps JC 1996 The structure of a complex of human 17 $\beta$ -hydroxysteroid dehydrogenase with estradiol and NADP<sup>+</sup> identifies two principal targets for the design of inhibitors. *Structure* 4:905–915
- Qiu W, Campbell RL, Gangloff A, Dupuis P, Boivin RP, Tremblay MR, Poirier D, Lin S-X 2002 A concerted, rational design of type 1 17 $\beta$ -hydroxysteroid dehydrogenase inhibitors: estradiol-adenosine hybrids with high affinity. *FASEB J* 16:1829–1831
- Petrow V 1986 The dihydrotestosterone (DHT) hypothesis of prostate cancer and its therapeutic implications. *Prostate* 9:343–361
- Labrie F, Dupont A, Belanger A, Giguere M, Lacoursiere Y, Emond J, Monfette G, Bergeron V 1985 Combination therapy with flutamide and castration (LHRH agonist or orchiectomy) in advanced prostate cancer: a marked improvement in response and survival. *J Steroid Biochem* 23:833–841
- Crawford ED 1989 Combined androgen blockade. *Urology* 34:22–26
- Labrie F, Belanger A, Cusan L, Labrie C, Simard J, Luu-The V, Diamond P, Gomez JL, Candas B 1996 History of LHRH agonist and combination therapy in prostate cancer. *Endocr Rel Cancer* 3:243–278
- Labrie F, Luu-The V, Lin S-X, Simard J, Labrie C, El-Alfy M, Pelletier G, Belanger A 2000 Intracrinology: role of the family of 17 $\beta$ -hydroxysteroid dehydrogenases in human physiology and disease. *Mol Endocrinol* 25:1–16
- Labrie F 2003 Extragonadal synthesis of sex steroids: intracrinology. *Ann Endocrinol (Paris)* 64:95–107
- Kuhn-Velten WN 2000 Intracrinology and the local enzymatic control of hormone distribution and metabolism: dehydroepiandrosterone does not just act as a prohormone for androgens and estrogens. *Eur J Clin Invest* 3:34–38

28. Sasano H, Suzuki T, Harada N 1998 From endocrinology to intracrinology. *Endocr Pathol* 9:9–20
29. El-Alfy M, Luu-The V, Huang X-F, Berger L, Labrie F, Pelletier G 1999 Localization of type 5 17 $\beta$ -hydroxysteroid dehydrogenase, 3 $\beta$ -hydroxysteroid dehydrogenase, and androgen receptor in the human prostate by *in situ* hybridization and immunocytochemistry. *Endocrinology* 140:1481–1491
30. Qin KN, Rosenfield RL 2000 Expression of 17 $\beta$ -hydroxysteroid dehydrogenase type 5 in human ovary: a pilot study. *J Soc Gynecol Investig* 7:61–64
31. Blouin K, Richard C, Belanger C, Dupont P, Daris M, Laberge P, Luu-The V, Tchernof A 2003 Local androgen inactivation in abdominal visceral adipose tissue. *J Clin Endocrinol Metab* 88:5944–5950
32. Labrie F, Luu-The V, Labrie C, Pelletier G, El-Alfy M 2000 Intracrinology and the skin. *Horm Res* 54:218–229
33. Penning TM, Burczynski ME, Jez JM, Lin HK, Ma H, Moore M, Ratnam K, Palackal N 2001 Structure-function aspects and inhibitor design of type 5 17 $\beta$ -hydroxysteroid dehydrogenase (AKR1C3). *Mol Cell Endocrinol* 171:137–149
34. Penning TM, Burczynski ME, Jez JM, Hung CF, Lin HK, Ma H, Moore M, Palackal N, Ratnam K 2001 Human 3 $\alpha$ -hydroxysteroid dehydrogenase isoforms (AKR1C1-AKR1C4) of the aldo-keto reductase superfamily: functional plasticity and tissue distribution reveals roles in the inactivation and formation of male and female sex hormones. *Biochem J* 351:67–77
35. Farber GK, Petsko GA 1990 The evolution of  $\alpha/\beta$  barrel enzymes. *Trends Biochem Sci* 15:228–234
36. Gangloff A, Shi R, Nahoum V, Lin S-X 2003 Pseudosymmetry of C19 steroids, alternative binding orientations, and multispecificity in human estrogenic 17 $\beta$ -hydroxysteroid dehydrogenase. *FASEB J* 17:274–276
37. Deleted in proof
38. Bennett MJ, Albert RH, Jez JM, Ma H, Penning TM, Lewis M 1997 Steroid recognition and regulation of hormone action: crystal structure of testosterone and NADP<sup>+</sup> bound to 3 $\alpha$ -hydroxysteroid/dihydrodiol dehydrogenase. *Structure* 5:799–812
39. Nahoum V, Gangloff A, Legrand P, Zhu D-W, Cantin L, Zhorov BS, Luu-The V, Labrie F, Breton R, Lin S-X 2001 Structure of the human 3 $\alpha$ -hydroxysteroid dehydrogenase type 3 in complex with testosterone and NADP at 1.25 Å resolution. *J Biol Chem* 276:42091–42098
40. Couture JF, Legrand P, Cantin L, Luu-The V, Labrie F, Breton R 2003 Human 20 $\alpha$ -hydroxysteroid dehydrogenase: crystallographic and site-directed mutagenesis studies lead to the identification of an alternative binding site for C21-steroids. *J Mol Biol* 331:593–604
41. Penning TM, Burczynski ME, Jez JM, Lin H-K, Ma H, Moore M, Ratnam K, Palackal N 2001 Structure-function aspects and inhibitor design of type 5 17 $\beta$ -hydroxysteroid dehydrogenase (AKR1C3). *Mol Cell Endocrinol* 171:137–149
42. Hoog SS, Pawlowski JE, Alzari PM, Penning TM, Lewis M 1994 Three-dimensional structure of rat liver 3 $\alpha$ -hydroxysteroid/dihydrodiol dehydrogenase: a member of the aldo-keto reductase superfamily. *Proc Natl Acad Sci USA* 91:2517–2521
43. Bennett MJ, Schlegel BP, Jez JM, Penning TM, Lewis M 1996 Structure of 3 $\alpha$ -hydroxysteroid/dihydrodiol dehydrogenase complexed with NADP<sup>+</sup>. *Biochemistry* 35:10702–10711
44. Jin Y, Stayrook SE, Albert RH, Palackal NT, Penning TM, Lewis M 2001 Crystal structure of human type III 3 $\alpha$ -hydroxysteroid dehydrogenase/bile acid binding protein complexed with NADP(+) and ursodeoxycholate. *Biochemistry* 40:10161–10168
45. Zhou M, Qiu W, Chang H-J, Gangloff A, Lin S-X 2002 Purification, crystallization and preliminary x-ray diffraction results of human 17 $\beta$ -hydroxysteroid dehydrogenase type 5. *Acta Crystallogr D* 58:1048–1050
46. Otwinowski Z, Minor W 1997 Processing of x-ray diffraction data collected in oscillation mode. *Methods Enzymol* 276:307–326
47. Kissinger CR, Gehlhaar DK, Fogel DB 1999 Rapid automated molecular replacement by evolutionary search. *Acta Crystallogr D* 55:484–491
48. Perrakis A, Morris R, Lamzin VS 1999 Automated protein model building combined with iterative structure refinement. *Nat Struct Biol* 6:458–463
49. Jones TA, Zou JY, Cowan SW, Kjeldgaard M 1991 Improved methods for binding protein models in electron density maps and the location of errors in these models. *Acta Crystallogr A* 47:110–119
50. Collaborative Computational Project Number 4 1994 The CCP4 suite: programs for protein crystallography. *Acta Crystallogr D* 50:760–763

